Exact study of lattice dynamics of single-walled carbon nanotubes

J. X. Cao,[1,2,*] X. H. Yan,[1] Y. Xiao,[1] Y. Tang,[1] and J. W. Ding[1,2]
[1]*Faculty of Material & Photoelectronic Physics, Xiangtan University, Xiangtan 411105, Hunan, China*
[2]*Institute of Mechanics and Material Engineering, Xiangtan University, Xiangtan 411105, Hunan, China*
(Received 20 August 2002; revised manuscript received 30 September 2002; published 30 January 2003)

Based on the model of lattice dynamics with force-constant matrix, we have calculated phonon spectrum and then specific heats of single-walled carbon nanotubes. The results show that with a more complicated phonon spectrum, a single-walled carbon nanotube has analogous good thermal conductivity to the two-dimensional graphite. However, the ratio of thermal conductivity to phonon relaxation time is inversely proportional to the diameter of either zigzag or armchair carbon nanotubes.

DOI: 10.1103/PhysRevB.67.045413 PACS number(s): 65.80.+n, 63.22.+m, 61.46.+w, 81.05.Uw

I. INTRODUCTION

Due to the development of micromanufacture technology accompanying by higher yield, lower cost, and better performance, the microelectronic devices have been continuously scaled down. The limits to the further miniaturization of microelectronics have led to intense research directed toward the development of nanoelectronics.[1] As a one-dimensional (1D) nanostructure material, single-walled carbon nanotubes (SWCN's) have been studied very well to hold extensive unique properties, such as controllable band structure, high mechanical strength, high thermal and chemical stability, and excellent heat conduction[2–8] for nanodevices in recent years. Various basic components composed of SWCN's such as diodes, [9] single-electron transistors,[10] field-effect transistors,[11] and primitive logic circuits[12] have been demonstrated recently. However, with the decrease in feature size and increase in power consumption, new challenges are turned up for device reliability, because thermal properties play critical roles in controlling the performance and stability of these devices.[13] Addressing these reliability issues requires better understanding of energy dissipation and thermal transport in these nanotube-based device components.

Fortunately, the unique structure of carbon nanotubes and stronger chemical bonds promise that an unusually high thermal conductivity of SWCN's would be expected in carbon nanotubes.[14,15] The strong $sp^{2+\delta}$ $(0\leqslant\delta\leqslant 1)$ bonds[7,8] in SWCN's give rise to high sound velocity in the range of 9–21×10^3 m/s.[4] In addition, scattering of phonons by boundary and defects is greatly reduced in a SWCN consisting of only one seamless and atomically perfect graphitic cylinder, resulting in long phonon mean free paths. Due to the high sound velocity and long phonon mean free paths, the thermal conductivity of SWCN's is expected to be extremely high. Recent experimental measurements[16–18] and molecular-dynamics simulations[19–21] have confirmed these predictions. The thermal conductivity of isolated SWCN's is suggested to be as high as 6600 W/mK at room temperature by nonequilibrium molecular-dynamics simulations.[19] Also, a high thermal conductivity of 1750–5800 W/mK is reported by experimental measurements[16–18] and the phonon mean free path is forecasted to be about 0.5–1.5 μm.[16] Although these studies[16–21] have yield a qualitative understanding of the intrinsic thermal properties of SWCN's, it is not sufficient to reveal the essential relationship between the unique structure and the special thermal properties. A problem is that these experimental studies only give an ensemble average over the different tubes in a mat sample. The measurement results, however, are difficult to interpret due to possibly deformed nanotubes and pockets of trapped voids in the mat samples. To find the mechanism of thermal transport comparative to the widely different estimations by the experimental measurements and numerical simulations, we develop lattice dynamics theory to study thermal properties of SWCN's. Some interesting calculations are obtained.

II. PRINCIPAL THEORY

For a three-dimensional crystal with primitive vectors $\mathbf{a}_1$, $\mathbf{a}_2$, $\mathbf{a}_3$, an atomic position is located at

$$\mathbf{R}(m,j)=\mathbf{r}(m)+\tau(j), \tag{1}$$

where $\mathbf{r}(m)=m_1\mathbf{a}_1+m_2\mathbf{a}_2+m_3\mathbf{a}_3$ (m_1,m_2,m_3 are integers) is the lattice vectors of mth unit cell and $\boldsymbol{\tau}(j)=j_1\mathbf{a}_1+j_2\mathbf{a}_2+j_3\mathbf{a}_3$ $(0\leqslant j_1,j_2,j_2\leqslant 1)$ is relative displacement in the unit cell. The potential Φ of lattice vibration can be expanded with Taylor series using the displacement $\mathbf{u}(m,j)$ of the atom in the properly unit cell as

$$\Phi=\Phi_0+\sum_{mj\alpha}\Phi_\alpha(m,j)u_\alpha(m,j) \tag{2}$$

$$+\frac{1}{2}\sum_{mj\alpha}\sum_{pk\beta}\Phi_{\alpha\beta}(mp,jk)u_\alpha(m,j)u_\beta(p,k)+\cdots, \tag{3}$$

in which $u_\alpha(m,j)(\alpha=1,2,3)$ is the displacement with respect to x,y,z direction, respectively. Φ_0 is the static potential and $\Phi_\alpha(m,j)$ is the force of the atom at balanceable location. The so-called force constant $\Phi_{\alpha\beta}(mp,jk)$, i.e., the coupling interaction coefficient between atom (m,j) and atom (p,k), is given by [28]

$$\Phi_{\alpha\beta}(mp,jk)=\frac{\partial^2\Phi}{\partial u_\alpha(m,j)\partial u_\beta(p,k)}. \tag{4}$$

One can easily find that $\Phi_{\alpha\beta}(mp,jk)=\Phi_{\beta\alpha}(pm,kj)$ from Eq. (4). The dynamics equation for the displacement of the jth atom in the unit cell can be written as[3,29]

$$M_j \ddot{u}_\alpha(m,j) = -\sum_{pk\beta} \Phi_{\alpha\beta}(mp,jk) u_\beta(p,k), \tag{5}$$

where M_j is the mass of the jth atom and α represents the displacement in direction of x,y,z, respectively. The vibrational wave functions of lattice vibration are often taken as

$$u_\alpha(m,j) = M_j^{-1/2} u_\alpha(j) e^{i[\omega t - \mathbf{q}\cdot\mathbf{r}(m,j)]}. \tag{6}$$

Substituting the wave function (6) into the dynamics equation (5), one obtains

$$\omega^2 u_\alpha(j) = \sum_{k\beta} F_{\alpha\beta}(jk,\mathbf{q}) u_\beta(k) e^{i[\mathbf{q}\cdot\boldsymbol{\tau}(j) - \mathbf{q}\cdot\boldsymbol{\tau}(k)]}, \tag{7}$$

where

$$F_{\alpha\beta}(jk,\mathbf{q}) = (M_j M_k)^{-1/2} \Sigma_p \Phi_{\alpha\beta}(mp,jk) e^{i\mathbf{q}\cdot[\mathbf{r}(m) - \mathbf{r}(p)]}$$

is the dynamical matrix element. From the dynamical equation, it is easy to obtain the secular equation of dynamics equation as

$$\det[\mathbf{F}(\mathbf{q}) - \omega^2 \mathbf{I}] = 0, \tag{8}$$

where $\mathbf{F}_{3j+\alpha,3k+\beta}(\mathbf{q}) = F_{\alpha\beta}(jk,\mathbf{q}) e^{i[\mathbf{q}\cdot\boldsymbol{\tau}(j) - \mathbf{q}\cdot\boldsymbol{\tau}(k)]}$. Solving the eigenvalue problem described as Eq. (8), we can get the phonon dispersion relations (PDR). In general, the vibrational density of states (VDOS) can be written as

$$g(\omega) = \frac{\Omega}{(2\pi)^3} \int \frac{dS}{|\nabla_q \omega(q)|} = \frac{\Omega}{(2\pi)^3} \sum_q \frac{\delta}{(\omega - \omega_q)^2 + \delta^2}, \tag{9}$$

where δ is the adjustable width factor of Lorentzian function.

After the PDR and VDOS are determined, the specific heat C_V at temperature T is given by the formula[22]

$$C_V(T) = \int_0^{w_{\max}} C_q(\omega) g(\omega) d\omega, \tag{10}$$

$$C_q(\omega) = k_B \left(\frac{\hbar\omega}{k_B T}\right)^2 \frac{\exp(\hbar\omega/k_B T)}{[\exp(\hbar\omega/k_B T) - 1]^2}, \tag{11}$$

where $C_q(\omega)$ is the thermal capacity of lattice wave with wave vector q and angular frequency ω. k_B and $\hbar$ are the Boltzmann constant and the Planck constant, respectively. And then the lattice thermal conductivity κ is defined by

$$\kappa = \sum_q \tau_{\lambda q} C_q(\omega_\lambda) v_{\lambda q}^2, \tag{12}$$

where λ is a set of quantum numbers specifying a phonon state. τ is the phonon relaxation time, v is the magnitude of the phonon group velocity along the direction of the heat flow.

III. RESULTS AND DISCUSSION

As a limited case, we calculate the PDR, VDOS, and the specific heat of the 2D graphite sheet as shown in Fig. 1. The primitive parameters of force constant can be obtained from Ref. 23. In Figs. 1 (a) and 1(b), the PDR and VDOS curves reproduce the experimental points obtained by electron energy-loss spectroscopy very well.[24,25] As expected, the specific heats per atom of 2D graphite sheet approach the

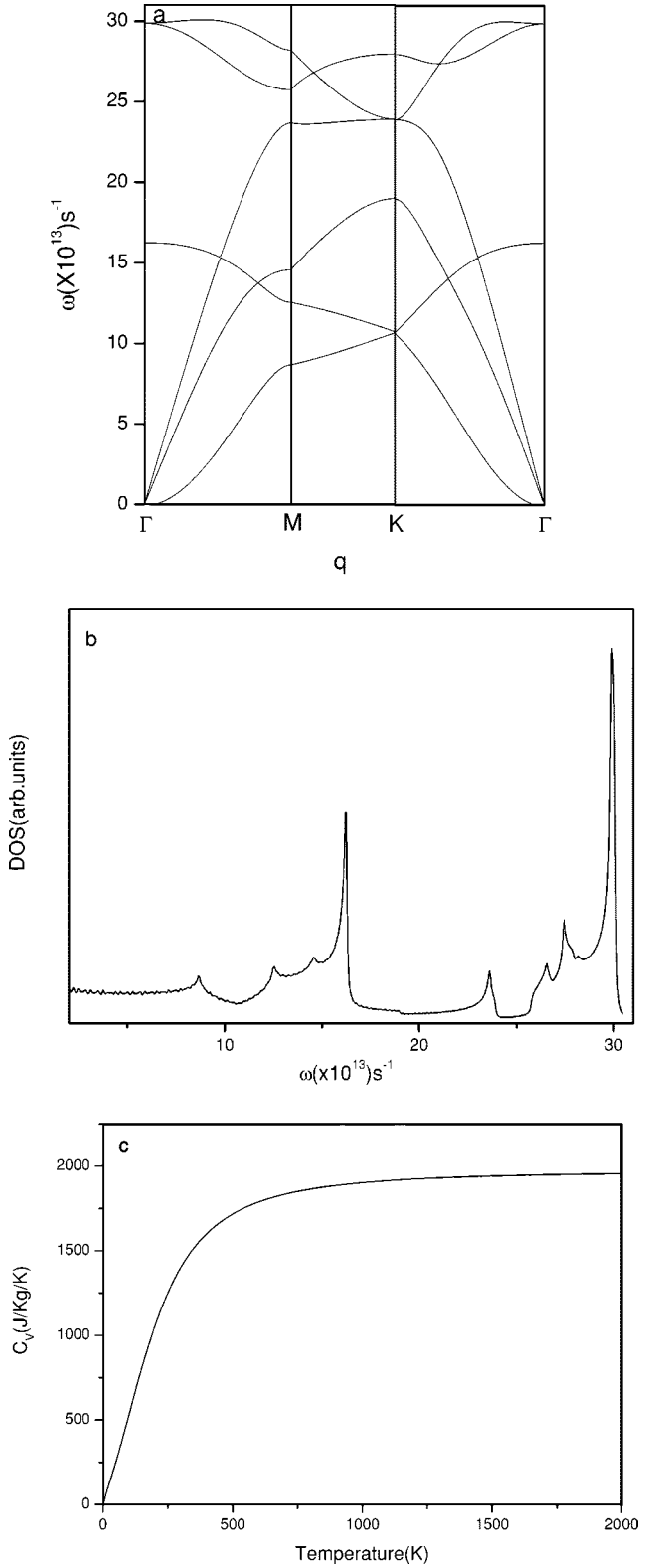

FIG. 1. Phonon dispersion relation (a), vibrational density of states (b), and specific heat (c) of 2D graphite sheet.

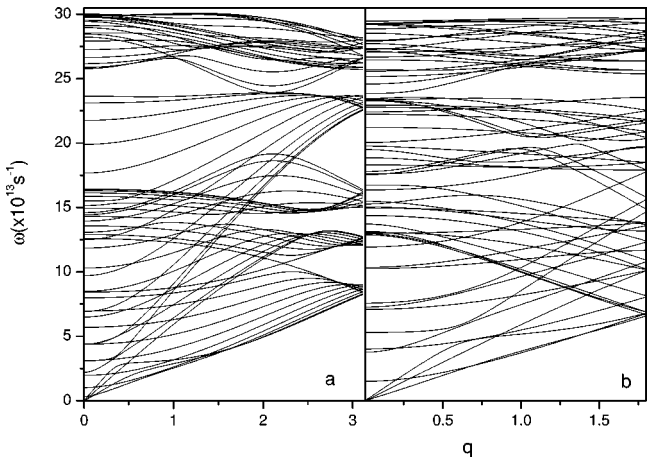

FIG. 2. Phonon dispersion relation of SWCN's in direction of tube axis. (a) For (10, 10) SWCN and (b) for (10, 0) SWCN's.

universal classical value of $3k_B$ in the high-temperature limit. However, a linear T dependence of C_V can be obtained at low temperature as shown in Fig. 1(c). It is believed to hold in our case, referring to the fact that a constant $g(\omega)$ at low frequency in a 2D system as shown in Fig. 1(b) would result in a linear T dependence of C_V.[26,27] For a flat graphite sheet, its hexagonal symmetry leads to a quadratically dispersed acoustic-phonon branch [see Fig. 1(a)], corresponding to the out-of-plane vibration mode of the sheet. This branch contributes to a constant term in $g(\omega)$ at low frequency.

After then, we apply the above dynamical theory to various types of SWCN's. The force-constant parameters were rescaled because of curvature effect of nanotubes.[3] In Figs. 2 and 3, we show PDR and VDOS for (10,10) and (10,0) SWCN with 40 atoms in each unit cell. Because of the mode degeneracies, there are only 66 distinct phonon branches, of which 12 modes are nondegenerate and 54 are doubly degenerate. The number of distinct phonon modes could be obtained by analysis of irreducible representation from space-group theory.[30] The first four modes of PDR around Γ point in Fig. 2 are acoustic modes, which include the doubly degenerated transverse acoustic modes, a longitudinal acoustic mode and a torsional acoustic mode. Roughly linear PDR curves for all these four phonon branches are obtained around Γ point. Similar to band structure of SWCN's,[6,7] the phonon structures split into many subbands because of the periodic boundary condition on the circumferential wave vector as demonstrated in Fig. 2. The VDOS for (10, 10) and (10, 0) SWCN's are shown in Figs. 3(a) and 3(b), respectively. One can find that the profile of VDOS curves for SWCN's is very similar to that of 2D graphite sheet. However, the VDOS curves for nanotubes is characterized with some bustling peaks in contrast to a constant and smooth curve for 2D graphite sheet at low frequency ($\omega < 10 \times 10^{13}\ s^{-1}$). Meaningly, the VDOS of SWCN's is proportional to the energy while a limited constant value for 2D graphite sheet at very low frequency. The corresponding VDOS of graphite sheet is greater in magnitude at $\omega = 0$ than that of a SWCN, because a graphite sheet is weak to bending, whereas a tube is markedly stiffer. At higher frequency ($10 \times 10^{13}\ s^{-1} \leqslant \omega \leqslant 17.5 \times 10^{13}\ s^{-1}$), the VDOS spectra of SWCN's extend and split. And it is apparently greater in magnitude than that of 2D graphite sheet. In addition, one can find that the VDOS of SWCN's is different from each other in Fig. 3. The spectrum of VDOS of (10, 0) SWCN is more sharp and narrow than that of (10, 10) SWCN. However, the profiles of VDOS of SWCN's and 2D graphite sheet are similar to each other although there exist many van Hove singularities at high frequency ($\omega \geqslant 17.5 \times 10^{13}\ s^{-1}$).

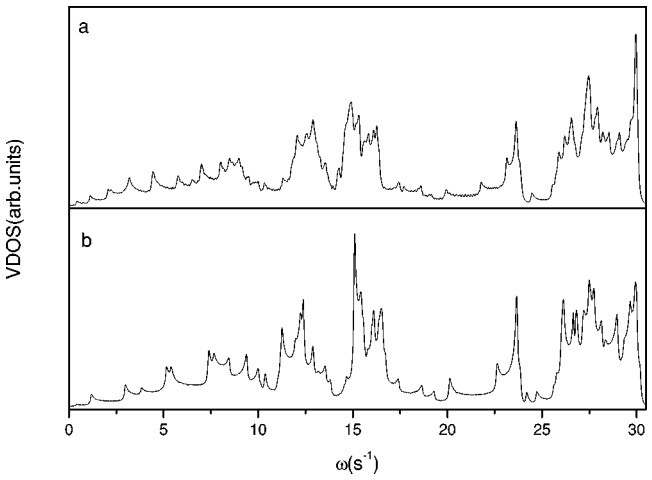

FIG. 3. Vibrational density of states of SWCN's (a) for (10, 10) SWCN's and (b) for (10, 0) SWCN's).

Figure 4 is connected with the specific heats $C_V(T)$ for (10, 10) and (10, 0) SWCN which are calculated from VDOS spectra according to Eq. (10). For comparison, the specific heat of 2D graphite is also shown. At very low temperature, $C_V(T)$ curves of SWCN's show the same character but lie well below the graphite one because the tube has no low-energy out-of-plane vibration modes. From the inset image of Fig. 4(a), one finds that the specific heat $C_V(T)$ of SWCN's increases monotonically with increasing T slowly at low temperature. The linearly dependence of T for $C_V(T)$ is consistent with analysis within Debye approximation for one-dimensional model. It may be reasonable that the thermal properties of SWCN show quasi-one-dimensional characters as the large ratio of length to diameter of SWCN's. The specific heat $C_V(T)$ increases dramatically above 30 K and arrives the universal classical value about 2077.4 J/(kg K) until about 1000 K. But for a 2D graphite sheet, $C_V(T)$ increases more rapidly as T increases. Such phenomenon attributes to the PDR (Fig. 2) and the VDOS (Fig. 3) of SWCN. At very low temperature, all the phonon modes of SWCN's except for the acoustic phonon are frozen out. Hence the specific heat increases slowly with increasing temperature. And when the temperature arrives at 30 K, the phonon in the first optical subband (the subband edge is at about 2.7 meV, or 30 K) (Ref. 16) is activated. It contributes to specific heat. Similar results can be obtained from other armchair nanotubes and zigzag nanotubes. But due to the first optical subband edge different from tube to tube, the turning points are diverse resulting in crossover of $C_V(T)$ curves as shown in Fig. 4(a). Although $C_V(T)$ curve of (10, 10) SWCN has same uptrend as that of (10, 0) SWCN at low

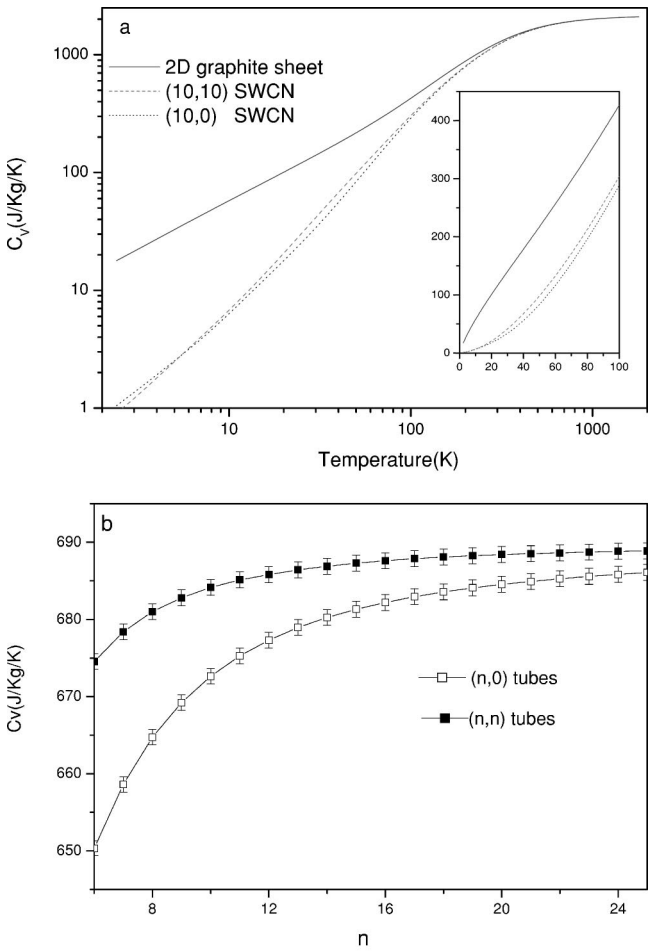

FIG. 4. (a) Temperature dependence of specific heats of SWCN's and 2D graphite sheet. (b) Specific heats of (n,n) SWCN's (line with triangle) and $(n,0)$ SWCN's (line with quadrangle) at 300 K.

temperature, it is greater in magnitude than that of (10, 0) SWCN because of the fatter VDOS of (10, 10) SWCN at higher temperature. But at about $T=700$ K, we have same value of specific heat $C_V(T)$ for (10, 10) SWCN, (10, 0) SWCN, and 2D graphite sheet. More detail calculations show that the specific heats of the same type SWCN's, i.e., zigzag tubes or armchair tubes, have similar character although their diameters are different from each other. Because the thermal properties like specific heat are integrated quantities over a wide frequency range and would be rather insensitive to the local spiky structures in VDOS. As shown in Fig. 4(b), the specific heats for zigzag tubes and armchair tubes increase as the diameter increase in exponential decay way at $T=300$ K. Fitting the data as function $C_V=C_V^0+Ae^{-r/r_0}$, we get parameters $C_V^0=688.71$ J/(kg K), $A=-70.21$ J/(kg K), $r_0=15.73$ Å for armchair tubes, and $C_V^0=685.88$ J/(kg K), $A=-144.61$ J/(kg K), $r_0=10.39$ Å for zigzag tubes. Interestingly, the specific heats of zigzag tubes is smaller than that of armchair tubes all along in spite of their diameters.

For convenience of calculations, we substitute the ratio $\tilde{\kappa}$ of the thermal conductivity to phonon relaxation time[22] for conductivity κ to descibe the thermal properties defined by

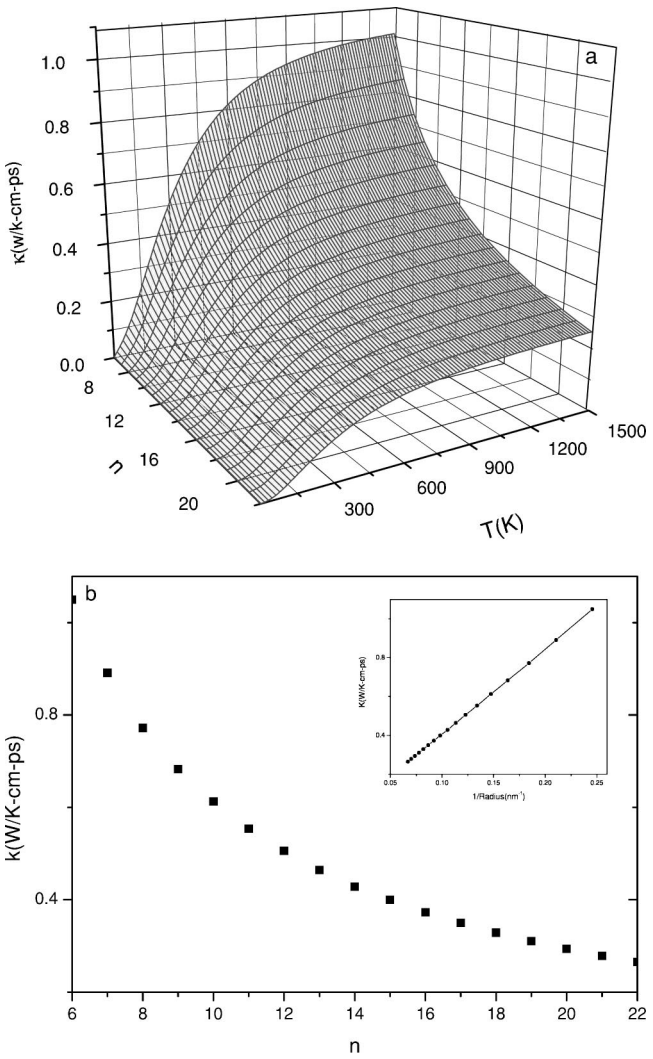

FIG. 5. (a) Temperature dependences of the ratio of thermal conductivity to phonon relaxation time of (n,n) SWCN's. (b) The ratio of thermal conductivity to phonon relaxation time of (n,n) SWCN's at 1500 K. The inset pattern shows the ratio of thermal conductivity to phonon relaxation time is inverse proportion of the diameter of SWCN's.

$$\tilde{\kappa}=\sum_{\lambda}\ \kappa_{\lambda}/\tau_{\lambda}=\sum_{\lambda}\ C_V(\omega)v_{\lambda q}^2. \tag{13}$$

In Figs. 5(a) and 6(a), the temperature dependence of the ratio $\tilde{\kappa}$ (per volume) for armchair SWCN's and zigzag SWCN's are shown, respectively. From the figures, one can learn that the magnitude of $\tilde{\kappa}$ is equivalent at very low temperature. However, the ratio $\tilde{\kappa}$ for the same type of SWCN's decreases as the diameter increase at high temperature. In addition, the magnitude of $\tilde{\kappa}$ for zigzag $(n,0)$ tubes is slightly greater relative to that for armchair (n,n) tubes. The curves in Figs. 5(a) and 6(b) also illuminate that ratios $\tilde{\kappa}$ increase rapidly with increasing temperature at low temperature. But the increasing speeds of the ratio vary from tube to tube. At high temperature, the speeds are depressed and the curves become aclinic. And the ratio $\tilde{\kappa}$ will approach a maxi-

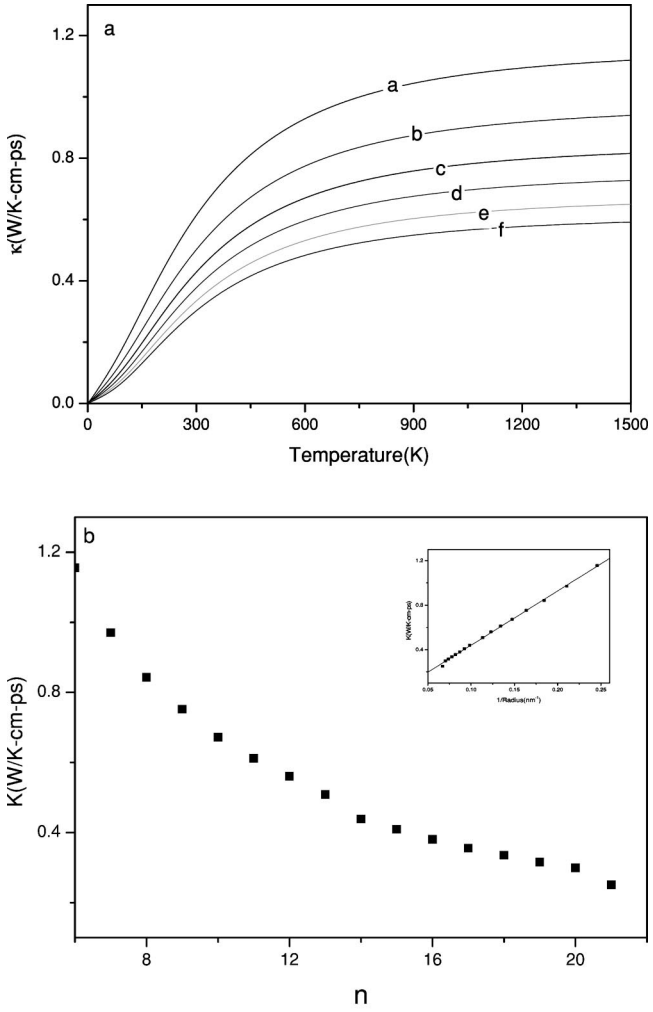

FIG. 6. (a) Temperature dependences of the ratio of thermal conductivity to phonon relaxation time of $(n,0)$ SWCN's (a)–(f) correspond to (6, 0) SWCN's–(11, 0) SWCN's, respectively. (b) The ratio of thermal conductivity to phonon relaxation time of $(n,0)$ SWCN's at 1500 K. The inset pattern shows the ratio of thermal conductivity to phonon relaxation time is inverse proportion of the diameter of SWCN's.

mum at temperature about 750 K although the maximal value of the ratio is different from tube to tube. The ratios $\tilde{\kappa}$ at 1500 K, corresponding with the maximum, of the armchair nanotubes and zigzag nanotubes are given in Figs. 5(b) and 6(b). The inset pattern in Figs. 5(b) and 6(b) shows that the ratio $\tilde{\kappa}$ of thermal conductivity to phonon relaxation time is inversely proportional to the diameter of SWCN's. Such phenomena might attribute to the phonon group velocity in SWCN. We show in Fig. 7 the frequency dependency of the square of the group velocity along the nanotube axis, defined by

$$\langle v^2(\omega)\rangle = \frac{1}{\Omega}\sum_{\lambda}\ \delta(\omega-\omega_{\lambda})v_{\lambda q}^2(\omega), \tag{14}$$

where $v_{\lambda q}(\omega)=\partial\omega_{\lambda}/\partial q$, $\delta(x)$ is delta function and Ω is volume of a SWCN. From Fig. 7, one can find that the

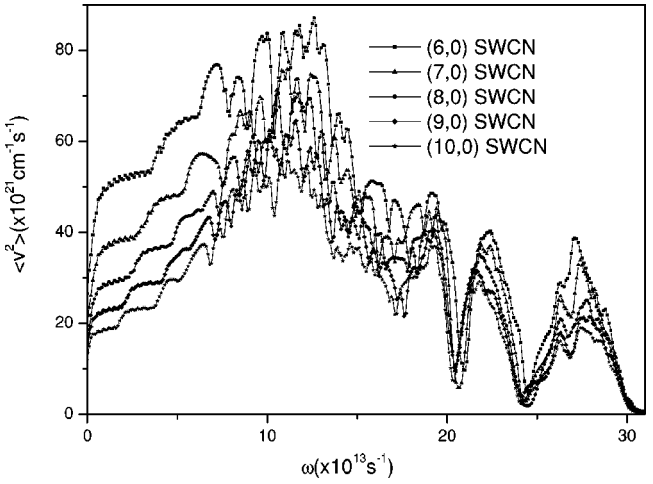

FIG. 7. The frequency dependence of the square of the phonon group velocity of zigzag nanotube along the tubule axis.

square of the group velocity decreases as the diameters of SWCN's increase. Consequently, the mean value of the group velocity is so small that they have no prominent effect on the heat conduction in SWCN's.

As nanodevice often works at room temperature, we pay our attention to the thermal properties for SWCN's at 300 K. As shown in Fig. 8, the ratio $\tilde{\kappa}$ at 300 K increases linearly as diameters of SCWN's decrease. Using linear fitting technique, we can obtain $\tilde{\kappa}=A/n$ with parameters $A=3.11\pm0.06$ W/K cm ps for armchair tubes and $A=3.84\pm0.08$ W/K cm ps for zigzag tubes. The results indicate that the thermal conductivity of (n,n) SWCN's is slightly smaller than that of $(n,0)$ SWCN's. This prediction is consistent with results by molecular-dynamics simulations.[20] Supposing that the phonon relaxation time is energy independent[16] in Eq. (12), we can evaluate the mean free path using the estimated magnitude of the thermal conductivity. A room-temperature thermal conductivity of 1750∼6600 W/mK (Refs. 16 and 19) implies that phonon mean free path $l\sim0.44$–1.55 μm, which is in agreement with experimental measurement.[16]

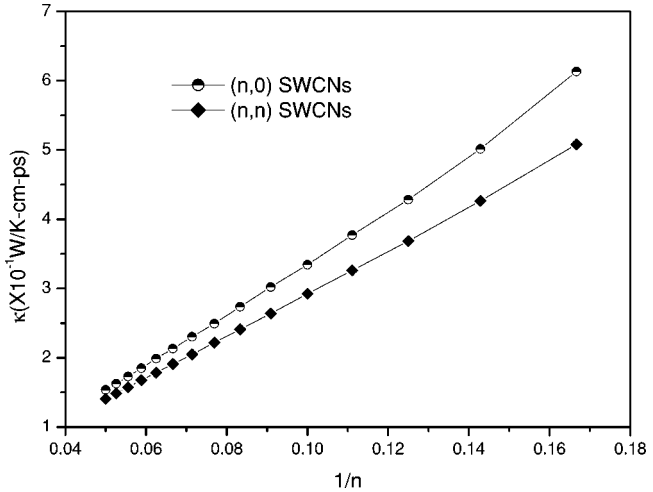

FIG. 8. The ratio of thermal conductivity to phonon relaxation time of $(n,0)$ SWCN's and (n,n) SWCN's at 300 K.

IV. CONCLUSIONS

Based on the model of lattice dynamics with force-constant matrix, we have calculated the PDR, VDOS, and the specific heats of SWCN's and estimated their contributions to the lattice thermal conductivity in direction of the tube axis. The results shows that the specific heats of SWCN's decrease linearly with decreasing the temperature at low temperature. This implies that thermal properties of SWCN's is dominated at all temperatures by phonons rather than by electrons. Moreover, the temperature-dependence ratio $\tilde{\kappa}$ of the thermal conductivity to phonon relaxation time decreases as the diameter of SWCN's increases and is inversely proportional to the diameter of SWCN's at high temperature. We found that the reduction of the group velocity yields the reduction in thermal conductivity. This implies that the group velocity of phonon makes a very significant contribution to thermal conductivity in SWCN's. In addition, we estimated the phonon meam free path of 0.44–1.55 μm for SWCN's at room temperature. More interestingly, the possibility of quantized thermal conductance at low temperature is suggested according to our calculated curves of frequency dependency of the square of the group velocity.

ACKNOWLEDGMENTS

This work was supported by National 973 Major Project Nanomaterials and Nanostructures (Grant No. 1999-0645-4500) and partly by the Science & Technology Foundation for Younger of Hunan Province (Nos. 00JJY2002 and 00JZY2138).

*Email address: caojuexian@263.net

[1] Y. Huang, X. F. Duan, Y. Cui, L. J. Lauhon, K.-H. Kim, and C. M. Lieber, Science **294**, 1313 (2001); G. Y. Tseng and J. C. Ellenbogen, *ibid.* **294**, 1293 (2001); P. G. Collins, A. Zettl, H. Bando, A. Thess, and R. E. Smalley, *ibid.* **278**, 100 (1997).

[2] X. Blase, L. X. Benedict, E. L. Shirley, and S. G. Louie, Phys. Rev. Lett. **72**, 1878 (1994).

[3] R. Saito, G. Dresselhaus, and M. S. Dresselhaus, *Physical Properties of Carbon Nanotubes* (Imperial College Press, London, 1998).

[4] R. Saito, G. Dresselhauls, and M. S. Dresselhaus, J. Appl. Phys. **73**, 494 (1993); M. S. Dresselhaus, G. Dresselhauls, and R. Saito, Solid State Commun. **84**, 201 (1992).

[5] C. T. White, D. H. Robertson, and J. W. Mintmire, Phys. Rev. B **47**, 5485 (1993); C. T. White and T. N. Todorov, Nature (London) **393**, 240 (1998).

[6] J. X. Cao, X. H. Yan, J. W. Ding, and D. L. Wang, J. Phys.: Condens. Matter **13**, L271 (2001).

[7] J. X. Cao, X. H. Yan, J. W. Ding, D. L. Wang, and Di Lu, J. Phys. Soc. Jpn. **71**, 1339 (2002).

[8] J. W. Ding, X. H. Yan, and J. X. Cao, Phys. Rev. B **66**, 073401 (2002).

[9] J. H. Schon, H. Meng, and Z. N. Bao, Science **294**, 2318 (2001).

[10] H. W. Ch. Postma, T. Teepen, Z. Yao, M. Grifoni, and C. Dekker, Science **293**, 76 (2001).

[11] J. Bonard, H. Kind, T. Stöckli, and L. Nilsson, Solid-State Electron. **45**, 893 (2001).

[12] A. Bachtold, P. Hadley, T. Nakenishi, and C. Dekker, Science **294**, 1317 (2001).

[13] S. Frank, P. Poncharal, Z. L. Wang, and W. A. De Heer, Science **280**, 1744 (1998).

[14] L. Wei, P. K. Kuo, R. L. Thomas, T. R. Anthony, and W. F. Banholzer, Phys. Rev. Lett. **70**, 3764 (1993).

[15] M. S. Dresselhaus, G. Dresselhaus, and P. C. Eklund, *Science of Fullerenes and Carbon Nanotubes* (Academic, San Diego, 1996).

[16] J. Hone, M. Whitney, C. Piskoti, and A. Zettl, Phys. Rev. B **59**, R2514 (1999); J. Hone, B. Batlogg, Z. Benes, A. T. Johnson, and J. E. Fischer, Science **289**, 1730 (2000).

[17] W. Yi, L. Lu, D. L. Zhang, Z. W. Pan, and S. S. Xie, Phys. Rev. B **59**, R9015 (1999).

[18] P. Kim, L. Shi, A. Majumdar, and P. L. McEuen, Phys. Rev. Lett. **87**, 215502 (2001).

[19] S. Berber, Y. Kwon, and D. Tommanek, Phys. Rev. Lett. **84**, 4613 (2000).

[20] M. A. Osman and D. Srivastava, Nanotechnology **12**, 21 (2001).

[21] J. W. Che, T. Cagin, and W. A. Goddard, III, Nanotechnology **11**, 65 (2000).

[22] S. I. Tamura, Y. Tanaka, and H. J. Maris, Phys. Rev. B **60**, 2627 (1999).

[23] R. A. Jishi, L. Venkataraman, M. S. Dresselhaus, and G. Dresselhaus, Chem. Phys. Lett. **209**, 77 (1993).

[24] T. Aizawa, R. Souda, S. Otani, Y. Ishizawa, and C. Oshima, Phys. Rev. B **42**, 11 469 (1990).

[25] C. Oshima, T. Aizawa, R. Souda, S. Otani, Y. Ishizawa, and Y. Sumiyoshi, Solid State Commun. **65**, 1601 (1988).

[26] R. Nicklow, N. Wakabayashi, and H. G. Smith, Phys. Rev. B **5**, 4951 (1972).

[27] K. Komatsu and T. Nagamiya, J. Phys. Soc. Jpn. **6**, 438 (1951); K. Komatsu, *ibid.* **10**, 346 (1955).

[28] V. N. Popov, V. E. Van Doren, and M. Balkanski, Phys. Rev. B **61**, 3078 (2000).

[29] R. Saito, T. Takeya, T. Kimura, G. Dresselhaus, and M. S. Dresselhaus, Phys. Rev. B **57**, 4145 (1998).

[30] O. E. Alon, Phys. Rev. B **63**, 201403(R) (2001).